Osteoporos Int (2014) 25:1735–1750
DOI 10.1007/s00198-014-2678-5

ORIGINAL ARTICLE

Effects of sequential osteoporosis treatments on trabecular bone in adult rats with low bone mass

S. K. Amugongo · W. Yao · J. Jia · Y.-A. E. Lay · W. Dai · L. Jiang · D. Walsh · C.-S. Li · N. K. N. Dave · D. Olivera · B. Panganiban · R. O. Ritchie · N. E. Lane

Received: 14 May 2013 / Accepted: 3 September 2013 / Published online: 11 April 2014
© International Osteoporosis Foundation and National Osteoporosis Foundation 2014

Abstract
Summary We used an osteopenic adult ovariectomized (OVX) rat model to evaluate various sequential treatments for osteoporosis, using FDA-approved agents with complementary tissue-level mechanisms of action. Sequential treatment for 3 months each with alendronate (Aln), followed by PTH, followed by resumption of Aln, created the highest trabecular bone mass, best microarchitecture, and highest bone strength.
Introduction Individual agents used to treat human osteoporosis reduce fracture risk by ~50–60 %. As agents that act with complementary mechanisms are available, sequential therapies that mix antiresorptive and anabolic agents could improve fracture risk reduction, when compared with monotherapies.
Methods We evaluated bone mass, bone microarchitecture, and bone strength in adult OVX, osteopenic rats, during different sequences of vehicle (Veh), parathyroid hormone (PTH), Aln, or raloxifene (Ral) in three 90-day treatment periods, over 9 months. Differences among groups were evaluated. The interrelationships of bone mass and microarchitecture endpoints and their relationship to bone strength were studied.
Results Estrogen deficiency caused bone loss. OVX rats treated with Aln monotherapy had significantly better bone mass, microarchitecture, and bone strength than untreated OVX rats. Rats treated with an Aln drug holiday had bone mass and microarchitecture similar to the Aln monotherapy group but with significantly lower bone strength. PTH-treated rats had markedly higher bone endpoints, but all were lost after PTH withdrawal without follow-up treatment. Rats treated with PTH followed by Aln had better bone endpoints than those treated with Aln monotherapy, PTH monotherapy, or an Aln holiday. Rats treated initially with Aln or Ral, then switched to PTH, also had better bone endpoints, than monotherapy treatment. Rats treated with Aln, then PTH, and returned to Aln had the highest values for all endpoints.
Conclusion Our data indicate that antiresorptive therapy can be coupled with an anabolic agent, to produce and maintain better bone mass, microarchitecture, and strength than can be achieved with any monotherapy.

Keywords Alendronate · Mass · Microarchitecture · Ovariectomy · Parathyroid hormone · Raloxifene · Strength

S. K. Amugongo · W. Yao · J. Jia · Y.-A. E. Lay · W. Dai · L. Jiang · D. Walsh · N. E. Lane (✉)
Center for Musculoskeletal Health and Department of Medicine, University of California Davis Medical Center, 4625 2nd Avenue, Suite 1002, Sacramento, CA 95817, USA
e-mail: nelane@ucdavis.edu

C.-S. Li
Division of Biostatistics, Department of Public Health Sciences, University of California, Davis, CA, USA

N. K. N. Dave · D. Olivera · B. Panganiban · R. O. Ritchie
Lawrence Berkeley National Laboratory, and Department of Materials Science and Engineering, University of California, Berkeley, CA, USA

Introduction

Osteoporosis is currently treated with effective therapies that act through different tissue-level mechanisms to reduce fracture risk. These include antiresorptive agents like bisphosphonates, a selective estrogen receptor modulator, and a receptor activator of NF kappa B ligand (RANKL) inhibitor, which reduce bone turnover [1], and an anabolic agent, parathyroid hormone (PTH; hPTH(1–34)) [2], which increases bone formation. Both antiresorptive and anabolic treatments, which may include both PTH(1–34) and PTH(1–84), raise bone mass, improve bone strength,

and reduce fracture risk in postmenopausal women with osteoporosis [3–6].

As osteoporosis is a chronic disease, long-term management is required. Though many patients respond well to treatment for a number of years, others may need additional therapy. As a result, osteoporosis medications with complementary tissue-level mechanisms of action are not infrequently prescribed in a sequential manner. As bisphosphonates are recommended as the first-line therapy for osteoporosis, many patients that may eventually receive PTH have already received bisphosphonates. Preclinical data that compare various treatment sequences could help guide future osteoporosis treatment strategies to achieve better fracture risk reduction than is possible with one agent alone.

Some clinical studies of sequential and/or combined treatment have been reported. PTH treatment has been followed by antiresorptive agents [7, 8]. Treatment with either raloxifene (Ral) or alendronate (Aln) has been followed by PTH [9, 10] or combined with PTH [10, 11]. Preclinical and clinical studies agree that sequential therapy using antiresorptive agents after PTH is necessary to maintain the bone mass that is added by PTH [7, 12–14]. However, all clinical studies of sequential osteoporosis treatments, not only are of relatively limited duration and sample size, but also lack fracture data. Most report only bone mineral density (BMD) data, which by itself is insufficient to completely predict fracture risk [15].

Studies have also been conducted using sequential therapy on small animal models of osteoporosis [14, 16, 17]. In rats that were ovariectomized (OVX) and left untreated for 11 weeks, the increased bone volume (BV) and trabecular BMD seen after 12 weeks of PTH(1–34), was lost within 12 and 24 weeks of PTH withdrawal, respectively [17]. When PTH withdrawal was followed by risedronate, both increased bone mass [17] and bone strength from PTH were maintained [18]. However, a dose of estrogen that prevented OVX-induced bone loss in adult female rats, failed to maintain BV/ total volume (TV), BMD, and bone strength, after PTH withdrawal [17].

Despite the fact that patients are now cycled through bone active medications, there are very few preclinical data addressing how these sequential osteoporosis therapies affect bone mass, microarchitecture, and strength. We propose to address with preclinical data, the possibility that properly sequencing current osteoporosis treatment agents, with their complementary mechanisms of action, can produce better fracture risk reduction than can be achieved by any single monotherapy. To do so, we evaluated bone quantity, microarchitecture, and strength in various sequences of antiresorptive and anabolic therapy that have already been or could be applied clinically. The goal of our study was to compare a set of preclinical bone endpoints from approved therapies in which fracture risk data exist for humans, to the same endpoints after sequential therapies in which human fracture risk has *not* yet been measured.

Materials and methods

Animals and experimental procedures

Six-month-old female OVX or sham-operated Sprague Dawley rats were purchased from and operated on at Harlan Laboratories (Livermore, CA, USA). The rats were shipped to our laboratory 2 weeks after surgery. They were then maintained on commercial rodent chow (Rodent Diet, cat. no. 2918, Teklad; Madison, WI, USA) in a 21ºC temperature room, with a 12-h light/dark cycle. Within a week of arrival in our laboratory, pair feeding of OVX to sham rats was started. Sham and OVX groups were necropsied at 2 months postsurgery (period 0). All remaining OVX rats were then randomized by body weight into ten groups (Table 1), which represent currently used and potential sequences of anti-osteoporosis medications. OVX rats were treated for 3 months (period 1) with vehicle (Veh; normal saline, 1 mL kg^{-1} $dose^{-1}$, three times per week by subcutaneous (SC) injection; Life Technologies, cat. no. 10010, Grand Island, NY, USA), PTH (hPTH(1–34) (human) acetate (25 μg kg^{-1} $dose^{-1}$ SC, 5×/week; Bachem Biosciences Inc, cat. no. H-4835, King of Prussia, PA, USA), Aln (25 μg kg^{-1} $dose^{-1}$ SC, 2×/week; Sigma, cat. no. A-4978, St. Louis, MO, USA), or Ral (5 mg kg^{-1} $dose^{-1}$, 3×/week by oral gavage; Sigma, cat. no. R-1402) (Table 1). No group was orally dosed three times weekly with Veh to control strictly for oral gavage of Ral rats.

The approved dose of PTH(1–34) for the treatment of human osteoporosis that is safe, well-tolerated, and efficacious, is 20 μg daily, equating to 2.3 μg kg^{-1} $week^{-1}$ in a 60-kg woman. A PTH(1–34) dose that is often used in rat studies is 80 μg/kg daily or 560 μg kg^{-1} $week^{-1}$ [19]. The PTH(1–34) dose of 25 μg kg^{-1} day^{-1} at 5 days/week utilized in our rat study is 125 μg kg^{-1} $week^{-1}$. As we administered PTH(1–34) for 90 days, we chose a dose that was only ~50-fold, rather than ~240-fold above that used in osteoporotic humans.

The approved dose for Ral for the treatment of human osteoporosis is 60 mg daily by mouth or 7 mg kg^{-1} $week^{-1}$ in a 60-kg woman. The Ral dose (5 mg/kg at 3 days/week) in our rat study is 2.1 mg kg^{-1} $week^{-1}$ orally. The minimum Ral dose that prevents most OVX-induced bone loss in rats is 1.5 mg kg^{-1} day^{-1} or 10.5 mg kg^{-1} $week^{-1}$ orally [20].

The approved dose of Aln for the treatment of human osteoporosis is 70 mg weekly by mouth or 1.17 mg kg^{-1} $week^{-1}$ in a 60-kg woman. Assuming a 0.7 % bioavailability, this equates to 8.2 μg kg^{-1} $week^{-1}$ that is absorbed. Our dose of Aln (50 μg kg^{-1} $week^{-1}$ SC) is also based on the minimum dose that has been reported to completely prevent OVX-induced bone loss in rats [21].

After 90 days (period 1), 6–12 animals were randomly selected from each group and necropsied, whereas the remaining animals were switched to their second treatment regimen.

Table 1 Experimental groups

Treatment group	Period 0 (days −60 to 0)	Period 1 (days 0–90)	Period 2 (days 91–180)	Period 3 (days 181–270)
Sham	No treatment (n=12)	No treatment (n=12)	No treatment (n=12)	No treatment (n=7)
OVX				
Veh-Veh-Veh	No treatment (n=10)	Vehicle (n=10)	Vehicle (n=10)	Vehicle (n=10)
Aln-Aln-Aln		Alendronate (n=12)	Alendronate (n=12)	Alendronate (n=12)
Ral-Ral-Ral		Raloxifene (n=11)	Raloxifene (n=11)	Raloxifene (n=12)
Aln-Veh-Aln		Alendronate (n=12)	Vehicle (n=12)	Alendronate (n=15)
PTH-Veh-Veh		hPTH(1–34) (n=12)	Vehicle (n=11)	Vehicle (n=12)
PTH-Aln-Veh		hPTH(1–34) (n=12)	Alendronate (n=12)	Vehicle (n=11)
PTH-Ral-Ral		hPTH(1–34) (n=6)	Raloxifene (n=12)	Raloxifene (n=12)
Aln-PTH-Veh		Alendronate (n=12)	hPTH(1–34) (n=12)	Vehicle (n=12)
Aln-PTH-Aln		Alendronate (n=11)	hPTH(1–34) (n=12)	Alendronate (n=10)
Ral-PTH-Ral		–	hPTH(1–34) (n=11)	Raloxifene (n=11)

Day −60 was the day of ovariectomy (OVX). Day 0 was the first day of dosing. Period 0 (days −60 to 0) allowed establishment of mild-moderate estrogen-deficiency osteopenia. OVX rats were still losing trabecular bone during periods 1 and 2. The number of rats killed after each period from each group is shown. As Ral treatment during period 1 was common to Ral-Ral-Ral and Ral-PTH-Ral groups, no rats from the Ral-PTH-Ral group were killed at the end of period 1. The treatment regimens were: Vehicle (Veh) subcutaneously (SC) at 1 mL kg^{-1} $dose^{-1}$, 3×/week; parathyroid hormone (hPTH(1–34)) (PTH) SC at 25 μg kg^{-1} $dose^{-1}$, 5×/week; alendronate (Aln) given SC at 25 μg kg^{-1} $dose^{-1}$, 2×/week; and raloxifene (Ral) by oral gavage at 5 mg kg^{-1} $dose^{-1}$, 3×/week

At 180 days, another 10–12 animals from each group were necropsied (period 2), whereas the remaining animals were switched to their third treatment for 90 days (period 3), at the end of which time they were necropsied. Experimental groups, with final numbers, are listed (Table 1). During the study, nine rats, randomly disbursed over the ten OVX groups, died, leaving 383 that reached necropsy. The study protocol was approved by the University of California Davis Institutional Animal Care and Use Committee.

At necropsy, the rats were euthanized by CO_2 inhalation. Whole blood was drawn by venipuncture of the left ventricle, then was transferred to a 10-cm^3 centrifuge tube and spun to yield serum that was then frozen at −20 °C. The uterus was inspected visually to confirm efficacy of OVX. The right femur and the lumbar vertebral (LV) spine 2–6 were excised and cleaned. The fifth lumbar vertebral body (LV5) and sixth lumbar vertebral body (LV6) were dissected free from the vertebral segment. The right femur and LV5 were placed in 10 % formalin for 24 h, and then transferred to 70 % ethanol. LV6 was wrapped in saline-soaked gauze and frozen at −20 °C. The right femur and LV5 were stored in 70 % ethanol, whereas LV6 remained at −20 °C until analysis.

MicroCT measurements of BV, microarchitecture, and degree of mineralization of bone tissue

The right distal femoral metaphysis (DFM) and LV5 were scanned with μCT (VivaCT 40, Scanco Medical AG, Bassersdorf, Switzerland) at 70 kev and 85 μA with a voxel size of 10.5 μm. Scanning of the DFM was initiated at the level of the growth cartilage-metaphyseal junction and extended proximally for 250 slices. Evaluations were performed on 150 slices beginning at 0.2 mm proximal to the most proximal point along the boundary of the growth cartilage with the metaphysis. The entire LV5 was scanned. All trabecular bone in the marrow cavity was evaluated. For each slice, the volume of interest was defined as ~0.25 mm internal to the boundary of the marrow cavity with the cortex. The methods for calculating BV, TV, trabecular thickness (Tb.Th), trabecular number (Tb.N), Structure Model Index (SMI), degree of anisotropy (DA), and degree of bone mineralization (DBM) have been described [22].

Biomechanical testing

Mechanical properties were determined by a compression test of the LV6. The posterior elements and transverse processes were removed with a bone cutter (Liston Gross Anatomy Bone Cutter, Fine Science Tools, Inc, cat. no. 16104, Foster City, CA, USA). The endplates were removed using a wafer saw and polished to flat, parallel surfaces. Before testing, seven measurements were taken using a digital caliper (Fowler® 0–12 in./300 mm IP54 Digital Caliper, Global Equipment Company, Inc, cat. no. T9FB799807, Buford GA, USA), that is, one length measurement (cranial-caudal direction) and six diameter measurements (major and minor axis at ~0.5 mm from the cranial end and the middle and at ~0.5 mm from the caudal end) of the vertebral body. The average diameter measurements were used with a standard area of a circle equation (π*((d/2)^2)), to calculate cross-sectional area of the test sample.

Test samples were stored in Hanks' balanced salt solution (HBSS) 12 h prior to testing. They were loaded using an electro servo-hydraulic materials testing system (MTS Model 831, Eden Prairie, MN, USA) in HBSS at 37 °C at a displacement rate of 0.01 mm/s. Maximum load, maximum stress, yield stress, stiffness, and energy absorption were calculated from the load-displacement curve. Energy absorption, or work to fracture, was specifically determined from the area under the load-displacement curve divided by twice the cross-sectional area of the test specimen.

Statistics

The group means and standard deviations (SDs) were calculated for all variables (Tables 2, 3, 4, and 5). In addition, when groups were treated identically during the same period, their data were combined and means and SDs for the combined data were calculated for all variables (Table 6). The differences for each variable between the two period 0 groups were analyzed by a two-sided *t* test. Differences among the eleven groups for each variable within periods 1, 2, and 3, respectively, were analyzed by analysis of variance (ANOVA). Differences were considered statistically significant at *p* value of ≤0.05 and intergroup differences were determined by an *F* test with the Bonferroni correction, as a post-hoc test for multiple (pair-wise) comparisons.

The relationship of BV/TV to SMI and DA in both the vertebral body and DFM was evaluated using linear regression. The bone mass, cross-sectional area, and microarchitectural endpoints that determine vertebral body maximum load were evaluated with multiple regression. All statistical analyses were performed with SAS v9.2 (Cary, NC, USA).

Table 2 Trabecular bone mass, microarchitecture, and bone strength at end of period 0

	Sham	OVX
MicroCT		
Number of rats	11	10
LV-BV/TV (%)	40.0±4.0*	27.8±4.7
LV-Tb.N (mm^{-1})	4.00±0.36*	3.36±0.31
LV-Tb.Th (μm)	90.4±4.8*	81.0±6.4
LV_SMI	−1.42±0.5*	−0.12±0.50
LV_DA	1.73±0.06	1.77±0.05
LV-DBM ($mgHA/cm^3$)	907±23*	871±15
Number of rats	11	8
DF-BV/TV (%)	31.3±4.0*	15.0±3.7
DF-Tb.N (mm^{-1})	4.84±0.49*	2.99±0.13
DF-Tb.Th (μm)	82.3±6.2*	72.4±6.7
DF_SMI	0.65±0.38*	1.88±0.20
DF_DA	1.42±0.05	1.46±0.08
DF-DBM ($mgHA/cm^3$)	970±14*	944±12
LV compression		
Number of rats	12	10
Max load (*N*)	210±46	180±51
Max stress (MPa)	21.0±4.2	17.8±4.0
Yield stress (MPa)	11.8±3.6	12.0±4.6
Stiffness (GPa)	0.55±0.23	0.40±0.16
Energy absorption (kJ/m^2)	5.1±2.5	3.9±1.9

Mean±SD

LV lumbar vertebral body, *DF* distal femur, *BV/TV* bone volume/tissue volume, *Tb.Th* trabecular thickness, *Tb.N* trabecular number, *SMI* Structure Model Index, *DA* degree of anisotropy, *HA* hydroxyapatite, *DBM* degree of bone mineralization, *Max load* maximum load, *Max Stress* maximum stress

*$p<.05$, difference from OVX

Results

The uteri in OVX rats were routinely observed to be smaller than those of sham rats at necropsy. Compared with sham, OVX resulted in a significant increase in body weight within 4 weeks of surgery ($p<0.05$). However, once pair feeding was begun, body weight in Veh-Veh-Veh rats dropped gradually and was not significantly different from sham rats at the end of any treatment period. Body weight was not affected by any treatment (data not shown).

BV and microarchitecture

Fifth lumbar vertebral body

At baseline and all subsequent time periods, lumbar vertebral body bone volume (LV-BV/TV) in Veh-Veh-Veh was less than in sham rats (Tables 2, 3, 4, and 5; Fig. 1a). At day 90, all treatment groups except for Ral-Ral-Ral, had higher LV-BV/TV than Veh-Veh-Veh (Table 3). Of the four groups that received Aln monotherapy in period 1, three (Aln-Aln-Aln, Aln-Veh-Aln, and Aln-PTH-Veh) had LV-BV/TV ranging from 32 to 36 %, whereas the fourth (Aln-PTH-Aln) had LV-BV/TV of 51 %, with a range in individual rats of 42–58 %, which was significantly different from the other three Aln-first groups (Fig. 1c). At day 180, LV-BV/TV in PTH-Veh-Veh was the same as Veh-Veh-Veh, whereas all other treatment groups were above Veh-Veh-Veh (Table 4; Fig. 1b). LV-BV/TV in PTH-Aln-Veh was higher than in all other treatment groups. By day 270, all regimens that included PTH, except for PTH-Veh-Veh and PTH-Ral-Ral, had greater LV-BV/TV than the other treatment groups (Table 5; Fig. 1b, c).

At all times, lumbar vertebral body trabecular number (LV-Tb.N) in Veh-Veh-Veh was less than in sham rats (Tables 2, 3, 4, and 5). At all times except day 90, lumbar vertebral body trabecular thickness (LV-Tb.Th) in Veh-Veh-

Table 3 Trabecular bone mass, microarchitecture, and bone strength at end of period 1 (day 90)

Group ID	Sham s	OVX *	Aln-Aln-Aln a	Ral-Ral-Ral b	Aln-Veh-Aln c	PTH-Veh-Veh d	PTH-Aln-Veh e	PTH-Ral-Ral f	Aln-PTH-Veh g	Aln-PTH-Aln h	Ral-PTH-Ral i
MicroCT											
Number of rats	12	10	12	11	12	12	12	6	12	12	
LV-BV/TV (%)	40.9±6.1*	28.7±5.2	32.2±3.0*bdefh	27.7±2.4cdefgh	33.4±3.5*defh	53.4±6.5*g	51.5±7.5*g	48.1±6.1*g	36.1±5.5*h	51.0±4.4*	
LV-Tb.N (mm^{-1})	4.09±0.54*	3.21±0.27	3.43±0.23*b	3.19±0.16cdefgh	3.54±0.25*	3.55±0.29*	3.50±0.36*	3.55±0.31*	3.42±0.19*	3.54±0.30*	
LV-Tb.Th (μm)	92.0±6.5	84.1±6.6	88.0±5.5*bdefh	81.7±4.6cdefgh	89.4±3.6*defh	139.5±15.5*g	134.0±11.4*g	121.7±10.2*g	97.5±12.5*h	132.4±6.4*	
LV-SMI	−1.71±0.78*	−0.35±0.55	−0.52±0.36*bdefh	−0.29±0.28cdefgh	−0.48±0.46*defh	−2.29±0.69*g	−2.84±1.14*g	−2.12±0.78*g	−0.90±0.58*h	−2.43±0.60*	
LV-DA	0.90±0.81*	1.76±0.07	1.75±0.07	1.71±0.04	1.76±0.04	1.67±0.11	1.69±0.08	1.67±0.04	1.73±0.09	1.67±0.08	
LV-DBM ($mgHA/cm^3$)	917±16*	887±13	887±15defh	904±17defh	901±18defh	936±20*egh	925±26*fgh	924±23*gh	908±31h	957±19*	
Number of rats	12	10	12	11	12	12	12	5	11	10	
DF-BV/TV (%)	29.4±7.0*	12.8±4.4	16.9±4.0bcdefh	8.5±2.8cdefgh	23.9±6.0*defh	39.4±6.2*gh	40.5±9.2*gh	34.5±4.4*gh	20.4±5.6*h	29.8±4.2*	
DF-Tb.N (mm^{-1})	4.62±0.53*	2.76±0.34	3.22±0.42*b	2.38±0.35*cdefgh	3.53±0.42*fgh	3.08±0.46*	3.37±0.58*h	2.97±0.22	2.90±0.45*	2.96±0.37*	
DF-Tb.Th (μm)	77.7±6.4	70.3±7.0	73.5±6.5bcdefgh	65.7±5.8cdefgh	83.8±7.9*defh	125.1±7.8*gh	122.3±8.6*gh	122.4±8.2*gh	89.1±16.1*h	112.9±5.6*	
DF-SMI	0.58±0.60*	1.96±0.45	1.76±0.21*bdefh	2.51±0.36*cdefgh	1.31±0.50*defh	−0.47±0.64*gh	−0.46±0.95*gh	0.07±0.41*gh	1.36±0.59*h	0.58±0.37*	
DF-DA	1.41±0.05	1.45±0.06	1.43±0.07defh	1.43±0.09defh	1.54±0.04defh	1.31±0.07*g	1.32±0.07*g	1.40±0.06*g	1.37±0.07h	1.29±0.06*	
DF-DBM ($mgHA/cm^3$)	967±20*	953±11	967±22*b	947±19cdefgh	972±13*	990±13*	983±17*	978±10*	983±23*	1,002±18*	
LV compression											
Number of rats	12	10	12	11	12	12	12	5	12	10	
Max load (*N*)	203±36	220±62	242±54bdefh	178±37cdefgh	213±23defh	357±51*fg	399±112*fgh	299±79*g	243±51h	318±72*	
Max stress (MPa)	20.4±2.8	19.9±4.0	20.8±3.5bdefh	17.5±3.0cdefgh	21.5±2.5defh	31.6±4.8*g	34.0±7.7*g	29.7±1.9*g	20.9±3.9h	27.2±4.7*	
Yield stress (MPa)	11.8±3.3	13.4±4.8	15.6±4.8defh	13.0±3.4defh	15.7±2.5defh	27.6±5.9*g	26.7±8.3*g	20.1±4.1*g	13.8±4.0h	22.7±5.2*	
Stiffness (GPa)	0.54±0.26	0.47±0.15	0.61±0.29*bde	0.48±0.17cdefgh	0.66±0.21*de	0.81±0.23*fgh	1.00±0.40*fgh	0.61±0.17*	0.61±0.19*	0.66±0.19*	
Energy absorption (kJ/m^2)	4.4±1.8	4.7±2.6	3.9±1.5bdef	7.1±3.4*cgh	5.4±2.8defg	8.0±3.8*gh	7.3±2.4*gh	7.5±1.1*gh	3.7±1.0	6.1±2.5	

Mean±SD. Lowercase letters—difference from group ($p<0.05$)

LV lumbar vertebral body, *DF* distal femur, *BV/TV* bone volume/total tissue volume, *Tb.N* trabecular number, *Tb.Th* trabecular thickness, *SMI* Structure Model Index, *DA* degree of anisotropy, *HA* hydroxyapatite, *DBM* degree of bone mineralization, *Max Load* maximum load, *Max stress* maximum stress

*$p<.05$, difference from OVX

Table 4 Trabecular bone mass, microarchitecture, and bone strength at end of period 2 (day 180)

Group ID	Sham s	OVX *	Aln-Aln-Aln a	Ral-Ral-Ral b	Aln-Veh-Aln c	PTH-Veh-Veh d	PTH-Aln-Veh e	PTH-Ral-Ral f	Aln-PTH-Veh g	Aln-PTH-Aln h	Ral-PTH-Ral i
MicroCT											
Number of rats	12	10	12	11	12	10	12	12	12	12	11
LV-BV/TV (%)	40.8±8.5*	18.1±2.5	32.6±3.5*deghi	28.9±3.8*deghi	33.6±3.5*deghi	22.2±1.9efghi	52.0±4.9*f	32.9±3.3*ghi	48.3±3.0*	50.6±4.1*	51.9±6.0*
LV-Tb.N (mm^{-1})	3.83±0.37*	2.80±0.25	3.39±0.19*bde	3.11±0.20*ceghi	3.43±0.18*df	2.96±0.17eghi	3.65±0.26*fgh	3.18±0.23*ghi	3.43±0.21*	3.43±0.21*	3.48±0.36*
LV-Tb.Th (μm)	97.9±15.9*	68.3±3.7	90.0±5.2*deghi	86.6±5.0*deghi	92.4±6.5*deghi	72.3±4.2efghi	133.7±8.5*f	91.5±4.5*ghi	136.2±5.8*	137.0±7.0*	138.2±7.4*
LV-SMI	−1.67±0.98*	0.61±0.30	−0.53±0.47*deghi	−0.33±0.41*deghi	−0.45±0.39*deghi	0.23±0.17efghi	−2.52±0.70*fgh	−0.70±0.35*ghi	−1.95±0.42*i	−2.15±1.67*i	−2.71±0.85*
LV-DA	1.67±0.06	1.74±0.07	1.75±0.08h	1.70±0.05	1.75±0.05	1.67±0.06	1.63±0.06	1.68±0.04	1.64±0.07	1.67±0.05	1.64±0.04
LV-DBM ($mgHA/cm^3$)	934±30*	857±12	892±12*bcdefghi	917±14*di	917±28*dei	860±5efghi	934±17*fi	911±14*i	923±13*i	926±17*i	959±16*
Number of rats	12	9	12	11	11	10	12	12	12	12	11
DF-BV/TV (%)	26.1±8.7*	6.2±3.3	13.8±2.3*ceghi	10.2±3.0cefghi	23.0±3.3*defghi	9.7±3.2efghi	35.7±5.5*f	17.5±4.7*ghi	32.3±3.9*i	33.5±4.2*i	34.8±4.3*
DF-Tb.N (mm^{-1})	4.23±0.54*	2.09±0.55	2.91±0.33*cdf	2.64±0.24*cegh	3.44±0.35*defi	2.39±0.23*eghi	3.10±0.37*f	2.46±0.44*ghi	3.17±0.30*i	3.17±0.30*i	2.82±0.28*
DF-Tb.Th (μm)	76.5±11.6*	60.9±4.9	71.6±4.2*cdefghi	66.3±6.6cefghi	84.3±5.9*deghi	62.8±7.0efghi	118.3±8.3*fi	82.9±4.9*ghi	115.8±7.1*i	114.3±5.5*i	128.3±5.2*
DF-SMI	0.69±0.76*	2.67±0.55	1.98±0.22*cefghi	2.32±0.35cefghi	1.49±0.21*deghi	2.03±0.42*efghi	−0.18±0.48*fgh	1.34±0.40*ghi	0.47±0.32*i	0.36±0.36*i	0.06±0.36*
DF-DA	1.41±0.07	1.38±0.06	1.44±0.06cdeghi	1.38±0.09ceghi	1.57±0.06*defghi	1.37±0.08eghi	1.28±0.05*f	1.41±0.08ghi	1.29±0.03*	1.31±0.05*	1.30±0.09*
DF-DBM ($mgHA/cm^3$)	970±19*	954±16	975±10*bdefi	956±15cdeghi	978±10*defi	937±19*efghi	1,004±17*fgh	958±11ghi	985±15*i	981±17*i	997±10*
LV compression											
Number of rats	12	10	12	9	12	11	12	12	12	11	8
Max load (*N*)	217±47	174±27	241±44*bcdefghi	188±42eghi	144±39deghi	190±36efghi	366±55*f	171±28ghi	368±87*i	387±50*i	332±28*
Max stress (MPa)	20.6±4.9*	14.5±1.1	20.9±4.0*cdefgh	17.6±3.5ceghi	11.8±4.3defghi	16.3±2.0eghi	30.5±3.4*f	16.8±2.2ghi	30.5±6.2*	31.7±4.4*	30.3±2.1*
Yield stress (MPa)	12.1±4.7	12.9±1.8	16.3±6.1cdefgh	12.6±2.6ceghi	6.6±3.4*defghi	11.6±3.9eghi	24.3±4.8*fhi	12.0±1.8ghi	24.2±3.5*i	26.3±5.1*i	19.1±1.6*
Stiffness (GPa)	0.66±0.27	0.52±0.23	0.68±0.28cde	0.62±0.15ce	0.29±0.13*efghi	0.47±0.15egh	0.89±0.34*fi	0.50±0.17gh	0.76±0.34*	0.86±0.35*	0.68±0.19
Energy absorption (kJ/m^2)	4.4±2.2*	2.1±0.9	3.7±2.3efghi	4.0±2.1efghi	3.9±1.4efghi	3.2±1.5efghi	7.2±2.6*hi	7.9±2.2*hi	5.8±2.4*i	6.9±3.6*i	10.1±4.7*

Mean±SD. Lowercase letters—difference from group ($p<.05$)

LV lumbar vertebral body, *DF* distal femur, *BV/TV* bone volume/total tissue volume, *Tb.N* trabecular number, *Tb.Th* trabecular thickness, *SMI* Structure Model Index, *DA* degree of anisotropy, *HA* hydroxyapatite, *DBM* degree of bone mineralization, *Max load* maximum load, *Max stress* maximum stress

*$p<.05$, difference from OVX

Table 5 Trabecular bone mass, microarchitecture, and bone strength at the end of period 3 (day 270)

Group ID	Sham s	OVX *	Aln-Aln-Aln a	Ral-Ral-Ral b	Aln-Veh-Aln c	PTH-Veh-Veh d	PTH-Aln-Veh e	PTH-Ral-Ral f	Aln-PTH-Veh g	Aln-PTH-Aln h	Ral-PTH-Ral i
MicroCT											
Number of rats	7	9	12	12	15	8	6	12	12	9	11
LV-BV/TV (%)	42.5±9.6*	20.6±3.5	33.0±2.5*bdeghi	27.2±2.9*cdefghi	31.8±4.1*deghi	20.3±3.3efghi	46.2±2.7*fghi	32.8±4.5*ghi	40.0±3.9*h	54.4±4.7*i	39.3±6.5*
LV-Tb.N (1/mm)	3.93±0.41*	2.78±0.27	3.34±0.15*bdh	3.00±0.27cdeghi	3.38±0.25*dfh	2.65±0.22efghi	3.53±0.13*fh	3.16±0.27*gh	3.48±0.28*h	3.85±0.30*i	3.26±0.29*
LV-Tb.Th (μm)	98.9±15.8*	71.0±4.3	89.7±5.5*deghi	84.2±2.9*defghi	89.1±4.4*deghi	73.2±4.2efghi	116.3±4.4*fgh	93.3±7.3*ghi	103.8±5.8*h	132.4±7.4*i	109.3±13.4*
LV-SMI	−1.97±1.02*	0.14±0.31	−0.65±0.26*degh	−0.30±0.31eghi	−0.32±0.39deghi	0.23±0.28efghi	−1.96±0.35*fghi	−0.71±0.36*fg	−1.33±0.38*h	−3.02±0.83*i	−1.17±0.62*
LV-DA	1.65±0.03	1.71±0.06	1.77±0.05	1.70±0.04	1.78±0.06	1.68±0.05	1.70±0.04	1.66±0.04	1.67±0.04	1.69±0.06	1.65±0.06
LV-DBM (mgHA/cm^3)	928±25*	886±18	931±16*bcdeh	908±18*eghi	912±16*degh	890±11efghi	955±26*fi	918±20*gh	937±15*h	970±23*i	927±22*
Number of rats	7	10	11	12	15	11	11	11	12	10	11
DF-BV/TV (%)	25.4±10.5*	6.8±1.9	14.4±3.2*bcdeghi	10.0±2.0cefghi	18.9±3.2*deghi	7.6±2.3efghi	26.5±3.7*fh	16.7±2.7*ghi	23.5±6.5*h	36.0±5.0*i	27.8±7.8*
DF-Tb.N (1/mm)	4.17±0.76*	2.28±0.24	2.91±0.30*bdfh	2.42±0.33cegh	3.23±0.34*dfi	2.11±0.32efghi	2.93±0.32*fh	2.51±0.25gh	2.99±0.56*h	3.42±0.23*i	2.75±0.43*
DF-Tb.Th (μm)	75.5±15.7*	64.0±4.3	73.1±3.6*eghi	72.7±4.0*cefghi	80.3±5.5*deghi	66.4±7.5efghi	97.7±7.8*fhi	80.7±4.1*ghi	91.8±7.4*hi	115.3±10.5*	110.6±23.5*
DF-SMI	0.74±0.80*	2.64±0.31	2.00±0.29*efghi	2.38±0.25cefghi	1.85±0.26*defghi	2.38±0.44efghi	0.68±0.34*fh	1.38±0.24*hi	1.04±0.48*hi	0.07±0.49*i	0.50±0.65*
DF-DA	1.41±0.06	1.37±0.08	1.47±0.06*bdeghi	1.41±0.07ch	1.50±0.04*deghi	1.41±0.12gh	1.35±0.05f	1.46±0.06*ghi	1.35±0.07	1.31±0.07	1.35±0.07
DF-DBM (mgHA/cm^3)	968±19	956±12	982±11*bdfh	968±10cdehi	987±13*dfg	953±16eghi	984±13*f	961±8hi	971±15*h	997±22*	989±31*
LV compression											
Number of rats	7	10	12	12	15	11	11	11	12	10	9
Max load (*N*)	255±68*	159±55	227±51*bcdegh	162±21eghi	171±47eghi	154±38efghi	282±45*fhi	205±43gh	275±51*hi	387±68*i	225±51*
Max stress (MPa)	21.9±6.0*	13.2±4.1	19.1±3.4*bcdegh	15.5±2.3efghi	15.2±4.3efghi	13.0±3.3efghi	23.6±3.2*fhi	20.2±4.0*h	22.7±3.4*h	31.6±3.8*i	19.8±4.5*
Yield stress (MPa)	15.5±4.1*	9.4±3.3	15.2±3.1*bcdh	10.8±2.3cefghi	7.3±2.0efghi	10.0±4.1efghi	15.3±3.0*h	15.2±3.9*h	17.5±4.2*h	23.8±6.1*i	15.3±4.8*
Stiffness (GPa)	0.73±0.24*	0.45±0.22	0.63±0.22cdh	0.44±0.14fh	0.37±0.13fgh	0.43±0.20fgh	0.53±0.16fh	0.73±0.27*	0.62±0.16h	0.86±0.25*i	0.55±0.22
Energy absorption (kJ/m^2)	4.5±1.8	2.9±2.7	3.3±1.3behi	5.3±1.7*cdi	3.2±2.0ehi	2.3±0.9efghi	7.1±2.3*fg	4.5±2.2hi	4.8±2.2i	6.5±2.0*	8.0±2.9*

Mean±SD. Lowercase letters—difference from group ($p<.05$)

LV lumbar vertebral body, *DF* distal femur, *BV/TV* bone volume/total tissue volume, *Tb.N* trabecular number, *Tb.Th* trabecular thickness, *SMI* Structure Model Index, *DA* degree of anisotropy, *HA* hydroxyapatite, *DBM* degree of bone mineralization, *Max load* maximum load, *Max stress* maximum stress

*$p<.05$, difference from OVX

Table 6 Data from Combinable Groups in periods 1 and 2

Variable	Aln-Aln-Aln, Aln-Veh-Aln, Aln-PTH-Veh, and Aln-PTH-Aln (period 1)	PTH-Veh-Veh, PTH-Aln-Veh, and PTH-Ral-Ral (period 1)	Aln-PTH-Veh and Aln-PTH-Aln (period 2)	Ral-Ral-Ral and Ral-PTH-Ral (period 1)
MicroCT				
Number of rats	47	30	24	11
LV-BV/TV (%)	37.9±8.5	51.6±6.9	47.0±4.9	27.8±2.4
LV-Tb.N (mm^{-1})	3.48±0.25	3.52±0.21	3.32±0.26	3.19±0.17
LV-Tb.Th (μm)	102.2±19.4	133.8±14.2	135.6±6.2	81.7±4.6
LV-SMI	−1.05±0.92	−2.48±0.93	−1.60±0.73	−0.29±0.28
LV-DA	1.73±0.08	1.68±0.09	1.66±0.07	1.71±0.04
LV-DBM ($mgHA/cm^3$)	912±34	929±23	924±15	904±17
Number of rats	45	29	24	11
DF-BV/TV (%)	22.5±6.8	39.0±7.5	32.9±4.0	8.5±2.8
DF-Tb.N (mm^{-1})	3.17±0.48	3.18±0.50	3.17±0.30	2.38±0.35
DF-Tb.Th (μm)	88.8±17.1	123.4±8.0	115.0±6.2	65.7±5.8
DF-SMI	1.29±0.58	−0.37±0.76	0.41±0.34	2.51±0.36
DF-DA	1.41±0.11	1.33±0.07	1.30±0.04	1.43±0.09
DF-DBM ($mgHA/cm^3$)	980±23	985±15	983±17	947±19
LV compression				
Number of rats	46	29	23	11
Max load (*N*)	251±62	364±91	377±71	178±37
Max stress (MPa)	22.4±4.4	32.3±5.9	31.1±5.3	17.5±3.0
Yield stress (MPa)	16.7±5.2	25.9±7.1	25.2±4.4	13.0±3.4
Stiffness (GPa)	0.63±0.22	0.86±0.33	0.81±0.34	0.48±0.17
Energy absorption (kJ/m^2)	4.73±2.06	7.60±2.85	6.32±3.02	7.08±3.38

Mean±SD

LV lumbar vertebral body, *DF* distal femur, *BV/TV* bone volume/total tissue volume, *Tb.N* trabecular number, *Tb.Th* trabecular thickness, *SMI* Structure Model Index, *DA* degree of anisotropy, *HA* hydroxyapatite, *DBM* degree of bone mineralization, *Max load* maximum load, *Max stress* maximum stress

Veh was less than in sham rats (Tables 2, 3, 4, and 5). At day 90, all treatment groups except for Ral-Ral-Ral, had higher Tb.N and Tb.Th than Veh-Veh-Veh (Table 3). Of the four groups that received Aln monotherapy in period 1, three (Aln-Aln-Aln, Aln-Veh-Aln, and Aln-PTH-Veh) had LV-Tb.Th that ranged from 88 to 97 μm, whereas the fourth (Aln-PTH-Aln) had LV-Tb.Th of 132 μm, with a range in individual rats of 125–141 μm, which was significantly different from the other three Aln-first groups. At day 180, all groups except for PTH-Veh-Veh had higher LV-Tb.N and LV-Tb.Th than Veh-Veh-Veh (Table 4). By day 270, all regimens that included PTH, except for PTH-Veh-Veh and PTH-Ral-Ral, had greater LV-Tb.N, and LV-Tb.Th than other groups (Table 5).

At all times, lumbar vertebral body degree of bone mineralization (LV-DBM) in Veh-Veh-Veh was less than in sham rats (Tables 2, 3, 4, and 5). At day 90, all groups except for Aln-Aln-Aln, Aln-Veh-Aln, Aln-PTH-Veh, and Ral-Ral-Ral had higher LV-DBM than Veh-Veh-Veh (Table 3). At day 180, LV-DBM in PTH-Veh-Veh was the same as Veh-Veh-Veh, whereas all other treatment groups were above Veh-Veh-Veh (Table 4). LV-DBM in Ral-PTH-Ral was higher than all other treatment groups (Table 4). By day 270, all regimens that included both PTH and Aln had greater LV-DBM than other treated groups, except for Ral-PTH-Ral and Aln-Aln-Aln (Table 5).

At all times, lumbar vertebral body Structure Model Index (LV-SMI) in Veh-Veh-Veh was higher than in sham rats (Tables 2, 3, 4, and 5). At day 90, though all PTH treatment groups had lower SMI than Veh-Veh-Veh, antiresorptive treatment alone did not affect SMI (Table 3). Of the four groups that received Aln monotherapy in period 1, three (Aln-Aln-Aln, Aln-Veh-Aln, and Aln-PTH-Veh) had LV-SMI that ranged from −0.48 to −0.9, whereas the fourth (Aln-PTH-Aln) had LV-SMI of −2.43, with a range in individual rats of −1.45 to −3.51, which was significantly different from the other three Aln-first groups. By day 180, LV-SMI in PTH-Veh-Veh was the same as Veh-Veh-Veh, whereas all other groups were significantly below Veh-Veh-Veh. In addition, LV-SMI in the antiresorptive only groups is significantly greater than LV-SMI in all groups that received PTH, except PTH-Ral-Ral (Table 4). At day 270, PTH-Veh-Veh was the only group whose LV-SMI did not differ from Veh-Veh-Veh. Antiresorptive only groups were significantly below Veh-Veh-

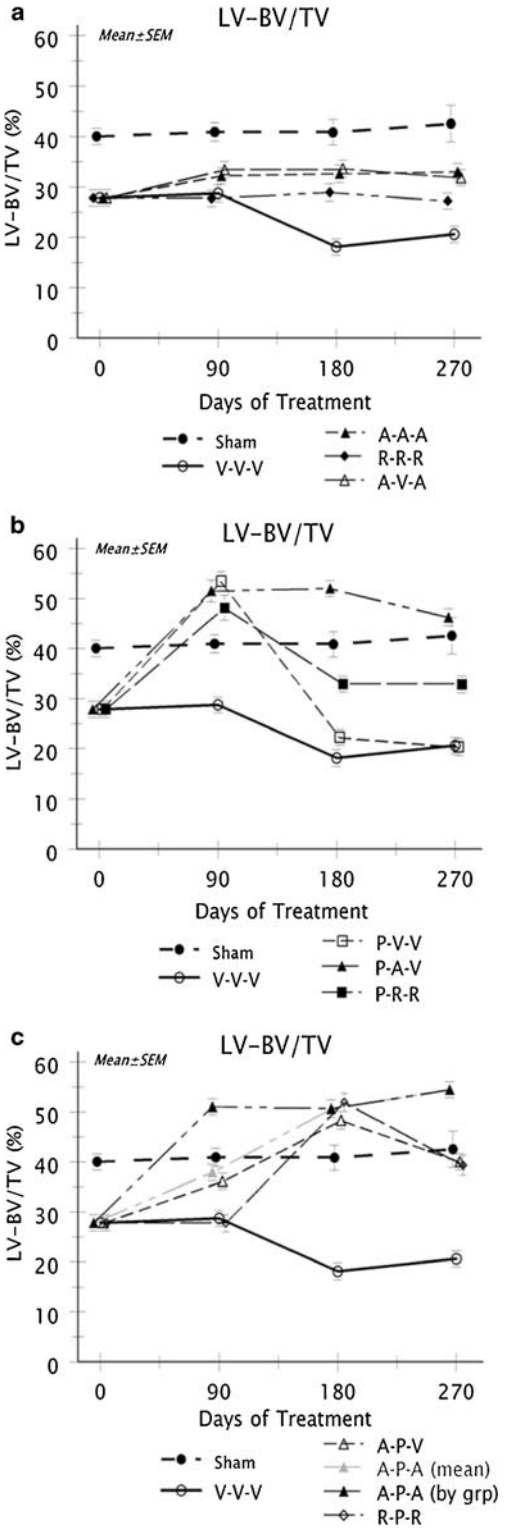

Fig. 1 These figures provide a graphical explanation of the study design and general outcome. The complete dataset with statistical testing is reported in Tables 2, 3, 4, and 5. The data represent individual groups of rats at each time period rather than longitudinal measurement of one set of rats. **a** LV-BV/TV data for all groups that received only antiresorptive monotherapy (A-A-A, R-R-R, and A-V-A) are shown. Sham and Veh-Veh-Veh group data are included for comparison. Veh-Veh-Veh rats had LV-BV/TV at ~30 % lower than that in sham rats at day 0, signaling established estrogen-deficiency osteopenia as treatments began. By day 270, osteopenia in Veh-Veh-Veh groups had progressed. Ral-Ral-Ral-treated groups did not develop additional osteopenia after day 90. Both Aln-Aln-Aln and Aln-Veh-Aln rats had significantly higher LV-BV/TV throughout the experiment than either Ral-Ral-Ral or Veh-Veh-Veh rats but never reached levels in age-matched sham rats. **b** LV-BV/TV data for all groups that received PTH(1–34) during period 1 (P-V-V, P-A-V, and P-R-R) are shown, along with sham and Veh-Veh-Veh data. All groups experienced a rapid increase in LV-BV/TV by day 90, which exceeded the sham levels, as PTH was given. Failure to follow up PTH cessation with antiresorptive therapy was associated with a rapid decline in LV-BV/TV, which reached Veh-Veh-Veh levels by day 180. Following up PTH cessation with Ral for 180 days was associated with significantly lower LV-BV/TV, which did not, however, reach the Veh-Veh-Veh level by day 270. Following up PTH cessation with Aln was associated with stable LV-BV/TV for 90 days. However, when Aln was stopped, a slow decline began that did not reach Veh-Veh-Veh levels by day 270 and was superior to levels seen with Ral maintenance. **c** LV-BV/TV data for groups that began with antiresorptive monotherapy, then switched to PTH (A-P-V, A-P-A, and R-P-R), are shown with sham and Veh-Veh-Veh data. The mean of all four groups that received ALN during period 1 is also plotted in *gray*. All treated groups experienced a rapid increase in LV-BV/TV between days 90 and 180, which exceeded sham levels, as PTH was administered. After PTH cessation, switching rats to Aln was significantly better than either switching to Ral or stopping all treatment. Unlike when PTH was given to treatment-naïve rats in period 1, when PTH was given to rats pretreated with antiresorptive monotherapy and then discontinued without follow-up treatment, LV-BV/TV did not return to Veh-Veh-Veh levels within 90 days

Veh, whereas groups that combined PTH with an antiresorptive had the lowest values for LV-SMI and were significantly lower than LV-SMI in the antiresorptive only groups. The lowest value was obtained in Aln-PTH-Aln at day 270 (Table 5).

Lumbar vertebral body degree of anisotropy (LV-DA) in Veh-Veh-Veh differed from sham only at day 90 (Table 2). There were no differences in LV-DA among all treatment groups at any time (Tables 3, 4, and 5).

Distal femoral metaphysis

At all times, distal femur bone volume (DF-BV/TV) in Veh-Veh-Veh was less than in sham rats (Tables 2, 3, 4, and 5). At day 90, all treatment groups except for Aln-Aln-Aln and Ral-Ral-Ral had higher DF-BV/TV than Veh-Veh-Veh (Table 3). At day 180, DF-BV/TV in PTH-Veh-Veh and Ral-Ral-Ral were not different from Veh-Veh-Veh, whereas all the other treatment groups were above Veh-Veh-Veh (Table 4). PTH-Aln-Veh, Aln-PTH-Veh, Aln-PTH-Aln, and Ral-PTH-Ral had greater DF-BV/TV than antiresorptive only groups (Table 4). By day 270, all regimens that included PTH, except for PTH-Veh-Veh, had greater DF-BV/TV than other treatment groups. Aln-PTH-Aln had greater DF-BVTV than any other group (Table 5).

At all times, distal femur trabecular number (DF-Tb.N) in Veh-Veh-Veh was less than in sham rats (Tables 2, 3, 4, and 5). At day 90, all groups except for Ral-Ral-Ral had higher DF-

Tb.N than Veh-Veh-Veh (Table 3). Furthermore, though all treatment regimens except Aln-Aln-Aln and Ral-Ral-Ral had higher DF-Tb.Th than Veh-Veh-Veh (Table 3), the greatest positive differences were seen in the PTH-treated groups that were greater than antiresorptive alone groups. By day 180, all treatment regimens had higher DF-Tb.N than Veh-Veh-Veh. All treatment regimens that included PTH except for PTH-Veh-Veh and PTH-Ral-Ral had higher DF-Tb.Th than Veh-Veh-Veh (Table 4). Antiresorptive groups that include Aln, but not Ral had significantly higher DF-Tb.Th than Veh-Veh-Veh. By day 270, Aln-Veh-Aln plus all regimens that included PTH, except for PTH-Veh-Veh and PTH-Ral-Ral had greater DF-Tb.N than other groups. By day 270, all regimens that included PTH, except for PTH-Veh-Veh and Ral-Ral-Ral, also had greater DF-Tb.Th than other treatment groups. Treatment groups that included both PTH and Aln, plus Ral-PTH-Ral, had the highest DF-Tb.N values (Table 5).

Before day 270, distal femur degree of bone mineralization (DF-DBM) in Veh-Veh-Veh was less than in sham rats (Tables 2, 3, 4, and 5). At day 90, all treatment groups except Ral-Ral-Ral had higher DF-DBM than Veh-Veh-Veh (Table 3). At day 180, DF-DBM in PTH-Veh-Veh, PTH-Ral-Ral and Ral-Ral-Ral was the same as Veh-Veh-Veh, whereas all other groups were greater than Veh-Veh-Veh (Table 4). DF-DBM in PTH-Aln-Veh was higher than all other treatment groups (Table 4). By day 270, PTH-Aln-Veh, Aln-Aln-Aln, Aln-Veh-Aln, Aln-PTH-Aln and Ral-PTH-Ral had greater DF-DBM than other groups (Table 5).

At all times, distal femur Structure Model Index (DF-SMI) in Veh-Veh-Veh was higher than in sham rats (Tables 2, 3, 4, and 5). At day 90, all treatment groups except for Aln-Aln-Aln and Ral-Ral-Ral had a lower DF-SMI than Veh-Veh-Veh. Groups that involved PTH treatment had the lowest DF-SMI values (Table 3). At day 180, all groups except for Ral-Ral-Ral had lower DF-SMI than Veh-Veh-Veh. The lowest DF-SMI values were in groups with both PTH and antiresorptive treatment (Table 4). By day 270, PTH-Veh-Veh and Ral-Ral-Ral no longer differed from Veh-Veh-Veh. The lowest values were found in groups that had received both PTH and antiresorptive treatment (Table 5).

Distal femur degree of anisotropy (DF-DA) in Veh-Veh-Veh did not differ from sham at any time (Table 2, 3, 4, and 5). At day 90, DF-DA in all regimens that included PTH was lower than the Veh-Veh-Veh group (Table 3). At day 180, DF-DA in PTH-Aln-Veh, Aln-PTH-Veh and Aln-PTH-Aln was less than Veh-Veh-Veh (Table 4). DF-DA in Aln-Veh-Aln was higher than all other groups. At day 270, Aln-Veh-Aln had greater DF-DA than all other groups (Table 5).

Mechanical testing (LV6)

At baseline and day 90, maximum load, maximum stress and yield stress in Veh-Veh-Veh did not differ from sham (Tables 2 and 3). At day 180, maximum stress in Veh-Veh-Veh was lower than in sham rats (Table 4). By day 270, maximum load, maximum stress, and yield stress were all lower in Veh-Veh-Veh than sham (Table 5). At day 90, all PTH regimens and Aln-PTH-Aln had higher maximum load, maximum stress, and yield stress than Veh-Veh-Veh. Of the four groups that received Aln monotherapy in period 1, three (Aln-Aln-Aln, Aln-Veh-Aln, and Aln-PTH-Veh) had maximum load that ranged from 213 to 243 N, whereas the fourth (Aln-PTH-Aln) had maximum load 318 N, with a range in individual rats of 217–473, that was significantly different from the other three Aln-first groups. The maximum load for the combined groups was 251±62 N (Table 6). By day 180, all PTH regimens, except PTH-Veh-Veh and PTH-Ral-Ral, had greater maximum load, maximum stress, and yield stress than the other groups. Though Aln-Veh-Aln strength did not different from Veh-Veh-Veh, all other groups that received Aln had maximum load, maximum stress and yield stress greater than Veh-Veh-Veh (Table 4). By day 270, Aln-Aln-Aln and all PTH-containing regimens, except for PTH-Veh-Veh had greater maximum load, maximum stress, and yield stress than other groups. Aln-PTH-Aln had the highest maximum load, maximum stress, and yield stress of all the groups (Table 5).

Intrinsic values for 3D microarchitectural variables

SMI and DA were measured in trabecular bone regions from over 350 samples each from the LV5 body and DFM. BV/TV ranged from 2.4 to 61.9 %. SMI ranged from −4.74 to +3.31 and DA ranged from 1.185 to 1.913. SMI was inversely and very strongly correlated to BV/TV (r=−0.954) (Fig. 2a). DA was about 20 % greater in the vertebral body than the DFM, and was weakly correlated to BV/TV in both sites (r=−0.289 and −0.346) (Fig. 2b).

Relationship of vertebral body maximum load to measurable vertebral body surrogate bone endpoints

Lumbar vertebral BV/TV, Tb.Th, and SMI were well-correlated to vertebral body maximum load, each explaining at least 55 % of the variation in maximum load (Table 7; Fig. 3). However, they were correlated to each other to such an extent that, in multiple regression (Table 8), Tb.Th, followed by cross-sectional area, with small contributions from DBM and SMI had the strongest association with maximum load. Together, these four endpoints explained 78 % of the variation in maximum load (Table 8). The correlation coefficient of maximum load to DA (r=−0.26) had a smaller absolute value than the correlation coefficients of maximum load to Tb.N, SMI, BV/TV, and Tb.Th, respectively (r=0.37–0.81) (Table 7).

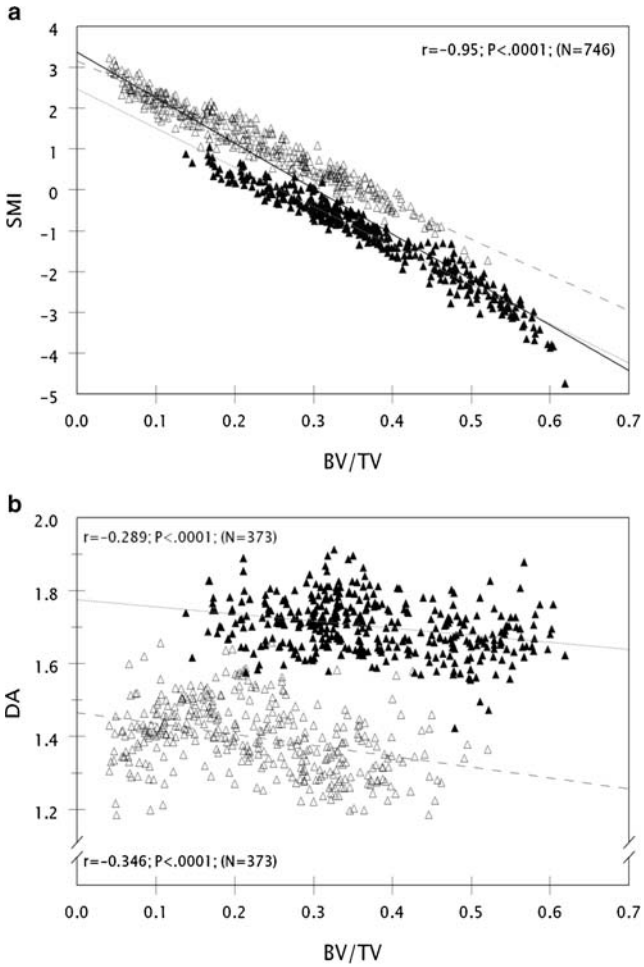

Fig. 2 **a** Data describing the relationship of SMI to BV/TV in 752 samples are plotted. Data from the lumbar vertebral body and DFM are plotted in *closed* or *open triangles*, respectively. Many specimens exhibit a negative SMI, particularly those with BV/TV greater than 0.3. There is a very strong negative linear relationship of SMI to BV/TV, whether considering all samples (r=0.954, *solid line*), vertebral body only (r=0.972, *dotted line*), or DFM only (r=0.971, *dashed line*). BV/TV explains over 91 % of the variation in SMI in the whole dataset. The y-intercepts for the vertebral body and distal femur differ, indicating that the vertebral body has a significantly more negative SMI for any BV/TV value than the DFM. **b** Data describing the relationship of DA to BV/TV in the vertebral body and DFM, respectively, are plotted as *closed* or *open triangles*. The vertebral body and DFM data are distinct populations, with the vertebral body being ~20 % higher than the distal femur. There is a weak negative linear relationship of DA to BV/TV in both the vertebral body only (r=0.289, *dotted line*) and DFM only (r=0.35, *dashed line*). The y-intercepts for the vertebral body and distal femur differ, indicating that the vertebral body has a significantly higher DA for any BV/TV value than the DFM

Discussion

Osteoporosis often requires medical treatment that continues for many years. No single currently approved medication begins to approach complete elimination of fracture risk. Fortunately, approved agents with complementary mechanisms of action are available. One could theorize that the systematic, sequential application of existing approved medicines that act strongly with complementary tissue-level actions can provide better fracture risk reduction than any single monotherapy.

Table 7 Correlation coefficients of maximum load to measurable bone endpoints in the lumbar vertebral body

Endpoint	*R*
BV/TV	0.768
Tb.Th	0.812
Tb.N	0.370
SMI	−0.742
DA	−0.263
DBM	0.477
Cross-sectional area	0.443

BV/TV bone volume/tissue volume, *Tb.Th* trabecular thickness, *Tb.N* trabecular number, *SMI* Structure Model Index, *DA* degree of anisotropy, *DBM* degree of bone mineralization

We investigated the effects of sequential treatment of osteopenic, OVX rats with complementary anti-osteoporosis agents on bone mass, bone microarchitecture, and bone strength endpoints. Each agent is efficacious by itself in reducing vertebral fracture risk in humans [2, 23, 24]. The first two categories of endpoints are generally known to be related to bone strength and provide a nondestructive, measurable surrogate for risk of fracture in humans. We examined all three categories of endpoints in OVX rats treated with each of the three agents as monotherapy. At the same time, we tested the monotherapies head to head against a series of sequences that have been or may be used in humans, again assessing the three categories of endpoints.

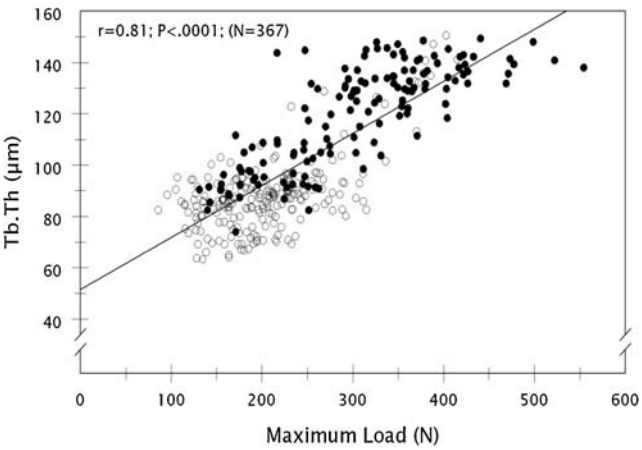

Fig. 3 Data describing the relationship of maximum load to Tb.Th in the vertebral body are plotted. Non-PTH- vs. PTH-treated rats killed immediately at the end of therapy or after antiresorptive maintenance are shown as *open* or *closed circles*, respectively. These data indicate a very strong relationship of Tb.Th to vertebral body maximum load, which is driven by treatment with PTH, producing trabecular bone regions with thicker trabeculae and lower SMI than in non-PTH-treated rats

Table 8 Determinants of maximum load (multiple regression) in the lumbar vertebral body

Endpoint	Total *R*
Tb.Th	0.812
Cross-sectional area	0.860
DBM	0.873
SMI	0.882

Tb.Th trabecular thickness, *DBM* degree of bone mineralization, *SMI* Structure Model Index

Our study started with 6-month-old OVX rats and allowed 8 weeks for development of estrogen-deficient osteopenia. Our data (Tables 2, 3, 4, and 5) show that estrogen-deficiency bone loss continued throughout the first two 3-month-treatment periods. As there was ongoing bone loss to prevent, this was a favorable environment for observing efficacy of antiresorptive monotherapy [21].

Physicians prescribe antiresorptive treatment as initial monotherapy for osteoporotic patients, because this treatment is proven to reduce fracture risk, and is safe, convenient, and cost-effective [23]. Accordingly, several treatment groups addressed such therapy and one even included a bisphosphonate "treatment holiday." Rats given continuous treatment with a bisphosphonate had better bone strength with modestly better bone mass and trabecular microarchitecture than untreated OVX rats. Though both the bisphosphonate drug holiday and continuous Ral groups had better bone mass, Tb.N, and Tb.Th than untreated OVX rats, these findings were not associated with better bone strength. As in humans, bisphosphonate treatment was associated with lower SMI [25]. Neither DBM nor SMI were as good in drug holiday and continuous Ral groups, as in the continuous Aln group. This may imply that the demonstrated relationship of DBM and SMI to bone strength (Table 7) is reflected in a practical way in the drug holiday and continuous Ral groups. Considering that bisphosphonate treatment increases DBM above that found in osteopenic subjects [26], some hypothesize that higher DBM accounts for a portion of the increased BMD and reduced fracture risk seen with antiresorptives [27]. Continuous antiresorptive therapy also improves the degree and uniformity of bone mineralization and maintains trabecular microstructure [28]. Our results for continuous Aln agree, showing better bone strength than in untreated OVX rats.

Clinical studies of fracture risk that include a bisphosphonate drug holiday have reported that fracture risk may rise, leading to recommendations that drug holidays be limited to patients with low or moderate fracture risk [29] and then only with intermittent monitoring for bone loss or fracture [30]. Our results show that despite better bone mass and microarchitecture in the drug holiday group than in untreated OVX rats, bone strength is *not* better. These preclinical data agree with reports that drug "holidays" may be associated with less antifracture efficacy than continuous bisphosphonate use. Our data also suggest that continuous bisphosphonate use provides better antifracture efficacy than continuous Ral. Though we increased our Ral dose by 150 % over one that was efficacious in a previous experiment [31], we cannot rule out that alternate day dosing of Ral may have contributed to this finding. It is known that 1.5 mg kg^{-1} $dose^{-1}$ daily Ral by oral gavage is the minimum dose that is sufficient to prevent most OVX-induced bone loss in adult rats [20].

Osteopenic, OVX rats treated with PTH had higher bone mass, better microarchitecture, and greater bone strength than untreated OVX rats at the end of PTH treatment. In particular, Tb.Th was 45–78 % higher and Tb.N was 8–22 % higher after PTH treatment, based on data from LV5 and the distal femur. However, these anabolic effects were completely lost within 3 months of PTH discontinuation, leaving the bone the same as untreated OVX rats, consistent with multiple preclinical and clinical studies [7, 32]. For example, PTH cessation in OVX rats caused trabecular bone loss that is detectable by 4 weeks with almost complete disappearance by 12 weeks [32]. Significant BMD loss is seen in postmenopausal women who receive placebo for 1 year after cessation of PTH [7].

PTH therapy is only approved by the FDA for a duration of 24 months [6]. For an individual patient, it is a matter of when, not if, PTH is discontinued. In agreement with other reports [7, 12, 13], our data show that post-PTH medical treatment must be provided to avoid loss of PTH's therapeutic benefit. Our study demonstrates that rats given PTH monotherapy followed by Aln monotherapy had better bone mass, microarchitecture, and strength than rats in which PTH was stopped without a follow-up treatment. These results are similar to those reported in clinical studies of PTH followed by a bisphosphonate or Ral [7, 12, 13]. We found that Aln was more efficacious than Ral in preserving PTH-related improvements in bone mass, microarchitecture, and strength. As previously mentioned, this may be related to our Ral dosing regimen. Other preclinical studies have investigated sequential therapies in OVX rats in which PTH was followed by estrogen [16], zoledronic acid [14], or risedronate [19]. These follow-up treatments resulted in lack of maintenance by estrogen replacement or maintenance with further gain in bone mass and strength with the bisphosphonates. Though the different times allowed from OVX to treatment initiation may play a role in the different findings, the strength of the antiresorptives employed may also be responsible. The data suggest that bisphosphonates are generally more efficacious at preserving PTH-related gains in bone strength than estrogen receptor binding antiresorptives. Our data indicate that initiating osteoporosis treatment with an anabolic agent then following up with bisphosphonate maintenance, could lead to better fracture risk reduction than either antiresorptive monotherapy or PTH treatment without follow-up maintenance.

In clinical practice, patients who fracture or lose bone while being treated with one medication require other therapeutic options. Preclinical data may guide those choices. We evaluated three groups that started with first-line therapy, then switched to PTH. Two of the three subsequently continued with the types of post-PTH maintenance tested previously here and discussed above.

All groups that switched to PTH from antiresorptive monotherapy had higher bone mass, higher Tb.Th, lower SMI, and higher bone strength immediately after the conclusion of treatment, than both untreated OVX rats and rats receiving continuous antiresorptives. The values were similar to those in rats that began PTH without prior use of antiresorptives, especially when considering the means of the combined groups with like treatment (Table 6). This indicates that prior antiresorptive treatment did not interfere with the skeleton's ability to respond positively to PTH, in agreement with previous preclinical findings [33].

Rats treated with PTH that was followed by no maintenance treatment, had lower bone mass, microarchitecture, and bone strength than rats that were switched to Aln maintenance therapy at the end of PTH treatment. Rats that switched to Ral maintenance had bone mass, microarchitecture, and bone strength similar to rats that had no post-PTH maintenance treatment. Another preclinical study that evaluated PTH combined with a Ral analog to treat osteopenia in OVX rats reported significant reduction in bone mass at several skeletal sites during Ral maintenance [34]. Though our results agree with other reports [34] that suggest a bisphosphonate is a better post-PTH maintenance therapy than Ral, we cannot rule out that our Ral dosing regimen influenced this finding.

At the end of study, rats treated sequentially with Aln, then PTH, and then Aln had the highest bone mass, microarchitecture, and bone strength of all the groups. These endpoints were at least as high as, and often higher than, sham rats. The Aln-PTH-Aln group at day 90 was significantly different from the other three day 90 groups treated with Aln for vertebral body endpoints. However, these are not the same rats that comprise the days 180 and 270 Aln-PTH-Aln groups. Therefore, these results need to be evaluated at the end of each treatment period (e.g., 90, 180, or 270 days) and not across the treatment periods. Our preclinical data suggest that a treatment plan that starts with a bisphosphonate, then switches to a period of PTH that significantly improves bone mass and microarchitecture, then switches to long-term bisphosphonate maintenance, is likely to have greater antifracture efficacy than any monotherapy. These results support the current choice of firstline therapy as antiresorptives, because one would predict that combining such therapy sequentially with an anabolic agent as needed, can provide more fracture risk reduction than can be achieved with either continuous frontline therapy or starting with PTH and then maintaining.

Our results provide additional practical data about SMI, an endpoint that describes the rod- or plate-like nature of trabecular lattices [35]. SMI has been thought to range mainly from zero to three, more negative values representing a more plate-like, stronger lattice [36, 37]. We found that, as in humans [38], PTH treatment reduced SMI. Though SMI here was very strongly and inversely correlated to BV/TV (Fig. 2a) [39, 40], almost half the specimens had negative SMI [36]. However, most existing SMI studies characterize samples from normal and osteopenic subjects with BV/TV in the range of 2–25 % [41] and report positive SMI [39, 42–44]. By contrast, one third of our specimens were from rats that had received efficacious treatment with anti-osteoporosis agents, which had BV/TV greater than 35 %. BV/TV was greater and SMI was more negative in the lumbar vertebral body than the DFM, but the values of the two bone sites were still highly correlated (Tables 2–5 and 9). Negative SMI indicates pores within high BV/TV trabecular lattices that have a structure with a concave surface [37]. Negative SMI has been seen in the proximal tibial epiphysis where BV/TV is 35–40 %, vs. the neighboring metaphysis where SMI is positive and BV/TV is 10–30 % [40]. The current data indicate that when specimens with high BV/TV are evaluated, SMI can be negative. SMI is an important determinant of bone strength (Table 7) [44, 45] and fracture risk [46], negative values being associated with the best strength.

Our data may provide additional insight into DA, an endpoint that describes the orientation of a trabecular lattice, with more positive values representing a more highly oriented trabecular lattice [35]. Unlike SMI, DA was not only weakly correlated to BV/TV (SMI r values of ~0.97 compared with mean *r* values of ~0.32), as reported previously [39, 43], but also did not consistently differ from controls in the treatment groups that had higher bone strength (Tables 2, 3, 4, and 5), as previously noted [47]. However, DA was about 20 % higher in vertebral bodies than in the DFM, indicating that the vertebral body trabecular lattice is more strongly oriented than that of the distal femur. Others have found that regions such as the tibial epiphyseal and metaphyseal trabecular bone, in which the epiphysis has higher BV/TV than the metaphysis, do not always have higher DA [47]. The current data combine with others' to suggest that DA describes fundamental properties of

Table 9 Correlation of microarchitectural endpoints of vertebral body to distal femoral metaphysis

Endpoint	*R*
Tb.Th	0.92
Tb.N	0.76
BV/TV	0.89
SMI	0.84

Tb.Th trabecular thickness, *Tb.N* trabecular number, *BV/TV* bone volume/tissue volume, *SMI* Structure Model Index

trabecular lattices from different anatomic regions [37], better than their BV or response to treatment.

We evaluated compressive strength of lumbar vertebral body specimens, in which maximum load ranged from 76–554 N. We also measured nondestructive descriptors of bone strength that included BV, Tb.N, Tb.Th, SMI, DA, cross-sectional area, and DBM. The endpoints themselves were highly correlated and therefore individually correlated to maximum load (Table 7). Tb.Th correlated best to maximum load (r=0.81, Fig. 3). Cross-sectional area, an endpoint independent of trabecular microarchitecture, added additional information. Our results suggest that, in rats treated with anti-osteoporosis agents, measuring microarchitectural and bone size endpoints of the lumbar vertebral body appears to be a nondestructive surrogate endpoint for vertebral body compression strength. The principal microarchitectural change affected by PTH treatment in this and other studies of both rats and humans, is trabecular thickening [38, 48] (Fig. 3). This probably explains the primary association of bone strength with Tb.Th here, rather than with SMI [45], and shows that trabecular thickening by an anti-osteoporosis treatment agent is a reasonable microarchitectural property of trabecular bone that can be used to predict bone strength after therapy, particularly with PTH. The results also agree with human data that suggest that bone mass and bone size in the spine predict spine fracture risk [49].

Our preclinical study had several strengths. We studied a number of clinical treatment sequences of bone active agents, measuring both nondestructive surrogate measures of bone strength and bone strength itself. We used 90-day treatment periods, approximately two remodeling periods in mature adult rats, that each may represent up to 12–24 months in humans. We evaluated treatments, such as monotherapy with a bisphosphonate, Ral, and PTH, for which clinical fracture risk-reduction data exist. We measured surrogate bone strength endpoints in both the approved monotherapies, and other sequences of treatment for which clinical fracture risk data have not yet been collected, to enable predictions about which ones could offer improved fracture risk reduction compared with monotherapy.

However, there were also weaknesses. The dosing regimen of Ral at 5 mg/kg, 3×/week, while reported to prevent estrogen-deficient bone in previous studies [26, 31], was both a lower dose and less frequent dosing than what has been reported to produce the maximum possible effect of Ral on prevention of OVX-induced bone loss [20]. Moreover, we cannot extrapolate our preclinical study results to osteoporotic fracture risk in humans. Since we began treatment at 8 weeks post-OVX, a time when OVX-related bone loss was still ongoing, the findings may be best applied to women who are within the first few years of menopause.

In summary, we used an osteopenic adult OVX rat model to evaluate various sequential treatments for osteoporosis, using FDA-approved agents with complementary tissue-level mechanisms of action. Sequential treatment for 3 months each with a bisphosphonate, followed by an anabolic agent, followed by resumption of the bisphosphonate, created the highest trabecular bone mass, highest Tb.Th, highest Tb.N, lowest SMI, and highest bone strength. Any type of drug holiday, particularly a PTH holiday, resulted in loss of bone strength. These data, if confirmed in clinical studies, may assist clinicians in the long-term treatment of postmenopausal osteoporosis.

Acknowledgments This work was funded by National Institutes of Health (NIH) grants R01 AR043052, 1K12HD05195801 and 5K24AR048841-09. Statistical support was made possible by grant no. UL1 RR024146 from the National Center for Research Resources (NCRR), a component of the NIH and NIH Roadmap for Medical Research. The involvement of ROR was supported by NIH (NIH/NIDCR) under grant no. 5R01 DE015633 to the Lawrence Berkeley National Laboratory (LBNL).

Conflicts of interest None.

References

1. Mackey DC, Black DM, Bauer DC, McCloskey EV, Eastell R, Mesenbrink P, Thompson JR, Cummings SR (2011) Effects of antiresorptive treatment on nonvertebral fracture outcomes. J Bone Miner Res: Off J Am Soc Bone Miner Res 26:2411–2418
2. Neer RM, Arnaud CD, Zanchetta JR et al (2001) Effect of parathyroid hormone (1–34) on fractures and bone mineral density in postmenopausal women with osteoporosis. N Engl J Med 344:1434–1441
3. Cummings SR, Karpf DB, Harris F, Genant HK, Ensrud K, LaCroix AZ, Black DM (2002) Improvement in spine bone density and reduction in risk of vertebral fractures during treatment with antiresorptive drugs. Am J Med 112:281–289
4. Cosman F, Keaveny TM, Kopperdahl D, Wermers RA, Wan X, Krohn KD, Krege JH (2014) Hip and spine strength effects of adding versus switching to teriparatide in postmenopausal women with osteoporosis treated with prior alendronate or raloxifene. Journal of bone and mineral research : the official journal of the American Society for Bone and Mineral Research (in press)
5. Lindsay R, Nieves J, Formica C, Henneman E, Woelfert L, Shen V, Dempster D, Cosman F (1997) Randomised controlled study of effect of parathyroid hormone on vertebral-bone mass and fracture incidence among postmenopausal women on oestrogen with osteoporosis. Lancet 350:550–555
6. Black DM, Bilezikian JP, Greenspan SL, Wuster C, Munoz-Torres M, Bone HG, Rosen CJ, Andersen HS, Hanley DA (2012) Improved adherence with PTH(1-84) in an extension trial for 24 months results in enhanced BMD gains in the treatment of postmenopausal women with osteoporosis. Osteoporos Int: J Established Result Cooper Bet Eur Found Osteoporos Natl Osteoporos Found USA 24:1503–1511
7. Black DM, Bilezikian JP, Ensrud KE, Greenspan SL, Palermo L, Hue T, Lang TF, McGowan JA, Rosen CJ (2005) One year of alendronate after one year of parathyroid hormone (1-84) for osteoporosis. N Engl J Med 353:555–565
8. Keaveny TM, Hoffmann PF, Singh M, Palermo L, Bilezikian JP, Greenspan SL, Black DM (2008) Femoral bone strength and its relation to cortical and trabecular changes after treatment with PTH,

alendronate, and their combination as assessed by finite element analysis of quantitative CT scans. J Bone Miner Res: Off J Am Soc Bone Miner Res 23:1974–1982
9. Ettinger B, San Martin J, Crans G, Pavo I (2004) Differential effects of teriparatide on BMD after treatment with raloxifene or alendronate. J Bone Min Res: Off J Am Soc Bone Miner Res 19: 745–751
10. Cosman F, Wermers RA, Recknor C, Mauck KF, Xie L, Glass EV, Krege JH (2009) Effects of teriparatide in postmenopausal women with osteoporosis on prior alendronate or raloxifene: differences between stopping and continuing the antiresorptive agent. J Clin Endocrinol Metab 94:3772–3780
11. Cosman F, Nieves JW, Zion M, Barbuto N, Lindsay R (2009) Retreatment with teriparatide one year after the first teriparatide course in patients on continued long-term alendronate. J Bone Miner Res: Off J Am Soc Bone Miner Res 24:1110–1115
12. Kurland ES, Heller SL, Diamond B, McMahon DJ, Cosman F, Bilezikian JP (2004) The importance of bisphosphonate therapy in maintaining bone mass in men after therapy with teriparatide [human parathyroid hormone(1–34)]. Osteoporos Int: J established Result Cooper Bet Eur Found Osteoporo Natl Osteoporos Found USA 15: 992–997
13. Rittmaster RS, Bolognese M, Ettinger MP, Hanley DA, Hodsman AB, Kendler DL, Rosen CJ (2000) Enhancement of bone mass in osteoporotic women with parathyroid hormone followed by alendronate. J Clin Endocrinol Metab 85:2129–2134
14. Rhee Y, Won YY, Baek MH, Lim SK (2004) Maintenance of increased bone mass after recombinant human parathyroid hormone (1-84) with sequential zoledronate treatment in ovariectomized rats. J Bone Miner Res: Off J Am Soc Bone Miner Res 19:931–937
15. Felsenberg D, Boonen S (2005) The bone quality framework: determinants of bone strength and their interrelationships, and implications for osteoporosis management. Clin Ther 27:1–11
16. Shen V, Birchman R, Xu R, Otter M, Wu D, Lindsay R, Dempster DW (1995) Effects of reciprocal treatment with estrogen and estrogen plus parathyroid hormone on bone structure and strength in ovariectomized rats. J Clin Investig 96:2331–2338
17. Iwaniec UT, Samnegard E, Cullen DM, Kimmel DB (2001) Maintenance of cancellous bone in ovariectomized, human parathyroid hormone [hPTH(1-84)]-treated rats by estrogen, risedronate, or reduced hPTH. Bone 29:352–360
18. Samnegard E, Akhter MP, Recker RR (2001) Maintenance of vertebral body bone mass and strength created by human parathyroid hormone treatment in ovariectomized rats. Bone 28:414–422
19. Li M, Mosekilde L, Sogaard CH, Thomsen JS, Wronski TJ (1995) Parathyroid hormone monotherapy and cotherapy with antiresorptive agents restore vertebral bone mass and strength in aged ovariectomized rats. Bone 16:629–635
20. Black LJ, Sato M, Rowley ER et al (1994) Raloxifene (LY139481 HCI) prevents bone loss and reduces serum cholesterol without causing uterine hypertrophy in ovariectomized rats. J Clin Investig 93:63–69
21. Seedor JG, Quartuccio HA, Thompson DD (1991) The bisphosphonate alendronate (MK-217) inhibits bone loss due to ovariectomy in rats. J Bone Miner Res: Off J Am Soc Bone Miner Res 6:339–346
22. Bouxsein ML, Boyd SK, Christiansen BA, Guldberg RE, Jepsen KJ, Muller R (2010) Guidelines for assessment of bone microstructure in rodents using micro-computed tomography. J Bone Miner Res: Off J Am Soc Bone Miner Res 25:1468–1486
23. Black DM, Schwartz AV, Ensrud KE et al (2006) Effects of continuing or stopping alendronate after 5 years of treatment: the Fracture Intervention Trial Long-term Extension (FLEX): a randomized trial. JAMA: J Am Med Assoc 296:2927–2938
24. Ettinger B, Black DM, Mitlak BH et al (1999) Reduction of vertebral fracture risk in postmenopausal women with osteoporosis treated with raloxifene: results from a 3-year randomized clinical trial. Multiple Outcomes of Raloxifene Evaluation (MORE) Investigators. JAMA: J Am Med Assoc 282:637–645
25. Recker RR, Ste-Marie LG, Langdahl B, Masanauskaite D, Ethgen D, Delmas PD (2009) Oral ibandronate preserves trabecular microarchitecture: micro-computed tomography findings from the oral iBandronate Osteoporosis vertebral fracture trial in North America and Europe study. J Clin Densitom: Off J Int Soc Clin Densitom 12:71–76
26. Yao W, Cheng Z, Koester KJ, Ager JW, Balooch M, Pham A, Chefo S, Busse C, Ritchie RO, Lane NE (2007) The degree of bone mineralization is maintained with single intravenous bisphosphonates in aged estrogen-deficient rats and is a strong predictor of bone strength. Bone 41:804–812
27. Burr DB, Miller L, Grynpas M, Li J, Boyde A, Mashiba T, Hirano T, Johnston CC (2003) Tissue mineralization is increased following 1-year treatment with high doses of bisphosphonates in dogs. Bone 33: 960–969
28. Rizzoli R, Chapurlat RD, Laroche JM, Krieg MA, Thomas T, Frieling I, Boutroy S, Laib A, Bock O, Felsenberg D (2012) Effects of strontium ranelate and alendronate on bone microstructure in women with osteoporosis. Results of a 2-year study. Osteoporos Int: J Established Result Cooper Bet Eur Found Osteoporos Natl Osteoporos Found USA 23:305–315
29. McClung M, Harris ST, Miller PD, Bauer DC, Davison KS, Dian L, Hanley DA, Kendler DL, Yuen CK, Lewiecki EM (2013) Bisphosphonate therapy for osteoporosis: benefits, risks, and drug holiday. Am J Med 126:13–20
30. Ro C, Cooper O (2013) Bisphosphonate drug holiday: choosing appropriate candidates. Curr Osteoporos Rep 11:45–51
31. Cheng Z, Yao W, Zimmermann EA, Busse C, Ritchie RO, Lane NE (2009) Prolonged treatments with antiresorptive agents and PTH have different effects on bone strength and the degree of mineralization in old estrogen-deficient osteoporotic rats. J Bone Miner Res: Off J Am Soc Bone Miner Res 24:209–220
32. Takano Y, Tanizawa T, Mashiba T, Endo N, Nishida S, Takahashi HE (1996) Maintaining bone mass by bisphosphonate incadronate disodium (YM175) sequential treatment after discontinuation of intermittent human parathyroid hormone (1–34) administration in ovariectomized rats. J Bone Miner Res: Off J Am Soc Bone Miner Res 11:169–177
33. Yao W, Su M, Zhang Q, Tian X, Setterberg RB, Blanton C, Lundy MW, Phipps R, Jee WS (2007) Risedronate did not block the maximal anabolic effect of PTH in aged rats. Bone 41:813–819
34. Hodsman AB, Watson PH, Drost D, Holdsworth D, Thornton M, Hock J, Bryant H, Fraher LJ (1999) Assessment of maintenance therapy with reduced doses of PTH(1–34) in combination with a raloxifene analogue (LY117018) following anabolic therapy in the ovariectomized rat. Bone 24:451–455
35. Stauber M, Muller R (2006) Volumetric spatial decomposition of trabecular bone into rods and plates–a new method for local bone morphometry. Bone 38:475–484
36. Hildebrand T, Ruegsegger P (1997) Quantification of bone microarchitecture with the Structure Model Index. Comput Methods Biomech Biomed Eng 1:15–23
37. Jiang Y, Zhao J, Liao EY, Dai RC, Wu XP, Genant HK (2005) Application of micro-CT assessment of 3-D bone microstructure in preclinical and clinical studies. J Bone Miner Metab 23(Suppl):122–131
38. Recker RR, Bare SP, Smith SY, Varela A, Miller MA, Morris SA, Fox J (2009) Cancellous and cortical bone architecture and turnover at the iliac crest of postmenopausal osteoporotic women treated with parathyroid hormone 1–84. Bone 44:113–119
39. Arlot ME, Burt-Pichat B, Roux JP, Vashishth D, Bouxsein ML, Delmas PD (2008) Microarchitecture influences microdamage accumulation in human vertebral trabecular bone. J Bone Miner Res: Off J Am Soc Bone Miner Res 23:1613–1618

40. Brouwers JE, van Rietbergen B, Huiskes R, Ito K (2009) Effects of PTH treatment on tibial bone of ovariectomized rats assessed by in vivo micro-CT. Osteoporos Int: J Established Result Cooper Bet Eur Found Osteoporos Natl Osteoporos Found USA 20:1823–1835
41. Brouwers JE, Lambers FM, Gasser JA, van Rietbergen B, Huiskes R (2008) Bone degeneration and recovery after early and late bisphosphonate treatment of ovariectomized wistar rats assessed by in vivo micro-computed tomography. Calcif Tissue Int 82:202–211
42. Borah B, Dufresne TE, Chmielewski PA, Johnson TD, Chines A, Manhart MD (2004) Risedronate preserves bone architecture in postmenopausal women with osteoporosis as measured by three-dimensional microcomputed tomography. Bone 34:736–746
43. Ito M, Nishida A, Nakamura T, Uetani M, Hayashi K (2002) Differences of three-dimensional trabecular microstructure in osteopenic rat models caused by ovariectomy and neurectomy. Bone 30:594–598
44. Teo JC, Si-Hoe KM, Keh JE, Teoh SH (2006) Relationship between CT intensity, micro-architecture and mechanical properties of porcine vertebral cancellous bone. Clin Biomech (Bristol, Avon) 21:235–244
45. Fields AJ, Eswaran SK, Jekir MG, Keaveny TM (2009) Role of trabecular microarchitecture in whole-vertebral body biomechanical behavior. J Bone Miner Res: Off J Am Soc Bone Miner Res 24: 1523–1530
46. Melton LJ 3rd, Christen D, Riggs BL, Achenbach SJ, Muller R, van Lenthe GH, Amin S, Atkinson EJ, Khosla S (2010) Assessing forearm fracture risk in postmenopausal women. Osteoporos Int: J Established Result Cooper Bet Eur Found Osteoporos Natl Osteoporos Found USA 21:1161–1169
47. Brouwers JE, Lambers FM, van Rietbergen B, Ito K, Huiskes R (2009) Comparison of bone loss induced by ovariectomy and neurectomy in rats analyzed by in vivo micro-CT. J Orthop Res: Off Publ Orthop Res Soc 27:1521–1527
48. Fox J, Miller MA, Newman MK, Metcalfe AF, Turner CH, Recker RR, Smith SY (2006) Daily treatment of aged ovariectomized rats with human parathyroid hormone (1–84) for 12 months reverses bone loss and enhances trabecular and cortical bone strength. Calcif Tissue Int 79:262–272
49. Melton LJ 3rd, Riggs BL, Keaveny TM et al (2007) Structural determinants of vertebral fracture risk. J Bone Miner Res: Off J Am Soc Bone Miner Res 22:1885–1892